VELOCITY PROFILE OPTIMIZATION FOR THE RIGA DYNAMO EXPERIMENT

F. STEFANI AND G. GERBETH
Forschungszentrum Rossendorf
P.O. Box 510119, D-01314 Dresden, Germany

AND

A. GAILITIS
Institute of Physics, Latvian Academy of Sciences
LV-2169 Salaspils 1, Riga, Latvia

Abstract. The Riga dynamo experiment is an attempt to show the self-excitation of a magnetic field in an electrically conducting fluid. Due to the absence of any scale separation effects, the precise shape of the velocity profile has a strong influence on the values of the critical magnetic Reynolds numbers (Rm). Several numerical codes have been developed and used for the determination of these critical Rm for arbitrary velocity profiles. Helicity maximizing profiles are shown to provide smaller critical Rm than the solid body rotation flow. We outline how the velocity profiles have been optimized in an iterative process including flow measurements, constructive improvements and numerical calculations.

1. Introduction

The magnetic fields of planets, stars and even galaxies are believed to be generated by the motion of electrically conducting fluids via the dynamo effect. Whereas the underlying theory has been elaborated in the last decades, experimental efforts are still rare. Notable is the successful experiment of Lowes and Wilkinson [1] with two rotating cylinders in a solid metal block. A first liquid metal experiment was undertaken in Riga in 1987 [2], [3]. Although the self-excitation threshold was not reached for reasons of mechanical instabilities the measured reaction of the system on an imposed magnetic field gave a clear indication of a possible dynamo effect at higher

flow rates.
From the viewpoint of flow topology, the present Riga experiment is very similar the the first one. Stimulated by the early work of Ponomarenko [4], the basic component of the facility consists of an axially symmetric helical flow of liquid sodium. In contrast to the Ponomarenko dynamo, this central helical flow is surrounded by a straight coaxial counterflow and an outermost cylinder with sodium at rest. This experimental arrangement enables not only a convective instability for the magnetic field self-excitation (as in the case of the Ponomarenko dynamo) but an absolute instability, too [2]. Calculating the critical Rm for a given geometry under the assumption of solid body rotation in the innermost cylinder, Gailitis [5] had estimated the sodium flow and the power necessary for magnetic field self-excitation.
However, a main problem of the Riga dynamo experiment is connected with the strong dependence of the critical Rm upon the shape of the velocity profile and with the difficulty to generate a desirable profile by means of a propeller and suitable guiding blades[1]. For example, the velocity profiles measured in a water pre-experiment [7] in 1996 differed remarkably from the solid body rotation (SBR)[2]. With these first profiles self-excitation of a magnetic field turned out to be clearly impossible with the installed motor power.
In this situation two problems arose. At first, it was indicated to look theoretically for velocity profiles yielding self-excitation with minimal power. At second, propellers and leading vanes had to be constructed in order to come close to those desirable profiles. The present paper outlines this process of velocity optimization.
In the second section the criterion of optimization is discussed. In order to compute the critical Rm for arbitrary profiles and to look for profiles with critical Rm as low as possible, we carried out a number of numerical simulations. In section 3 we describe a simple finite difference solver for the time-dependent induction equation in one dimension (1D), taking into account only the first azimuthal component and fixed Fourier components in z-direction. Some of the results have been verified by comparison with the outcomes of an eigenvalue equation solver. Additionally, a two-dimensional (2D) code was developed and used in order to check the effects of the finite length of the system and of possible variations of the velocity profiles along the z-axis. This code is presented in section 4. In section 5 the calculated critical Rm are given for several theoretical as well as measured velocity profiles. Helicity maximizing profiles are shown to provide lower critical Rm

[1]This is in contrast to the Karlsruhe experiment, where the precise shape of the velocity profile plays only a negligible role due to the effect of scale separation [6].

[2]The notation "solid body rotation" is defined here by a radial dependence of the axial and the azimuthal velocity components according to $v_z(r) \sim const$ and $v_\phi(r) \sim r$.

than the solid body rotation flow. The process of technical improvements of the facility leading to satisfying velocity profiles is reported.

2. Optimization Criterion

The full optimization of a whole dynamo experiment is a very complex project. Supposing a certain relation of construction costs and operating costs, Gailitis [5] had optimized in a first step the basic geometric relations of the facility. Figure 1 shows the resulting dimensions and the basic components of the experimental setup.
First experiments at a water dummy channel had shown a remarkable deviation of the measured velocity profiles from the solid body rotation profiles supposed in former calculations. At the same time, preliminary computations had indicated a strong dependence of the critical Rm on the shape and the relative strengths of the azimuthal velocity v_ϕ and the axial velocity v_z. It turned out that in order to achieve self-excitation for given power resources a change of the velocity profiles was unavoidable.
The first difficulty for a velocity profile optimization applies to a reasonable definition of the optimization criterion. In a technical sense, it would be desirable to find velocity profiles which require minimal power for the self-excitation of a magnetic field. However, the determination of the necessary power would represent an enormous hydrodynamic task for its own. An easier task is to look for velocity profiles with a minimal critical Rm. But even the definition of Rm is to some extent arbitrary. In the following we use the definition

$$Rm = \mu\sigma \; R_1 \sqrt{\overline{{v_z}^2} + 2\,\overline{{v_\phi}^2}} \; . \tag{1}$$

By virtue of the averaging

$$\overline{{v_*}^2} = \frac{2}{R_1^2} \int_0^{R_1} {v_*}^2(r)\, r dr \tag{2}$$

over the radius R_1 of the innermost cylinder, this definition has regard to the integral properties of the flow and not only to the maximal velocity. The stronger weighting of $\overline{{v_\phi}^2}$ is motivated by the fact that for a solid body rotation the major part of the losses comes from the boundary region. For this special case, our definition is equivalent to the often used definition $Rm = \mu\sigma R_1 v_{max}$ based on the maximum value of the velocity. According to the definition of Rm, we define the pitch parameter κ as

$$\kappa \;\; = \;\; \sqrt{\frac{\overline{{v_z}^2}}{2\,\overline{{v_\phi}^2}}} \tag{3}$$

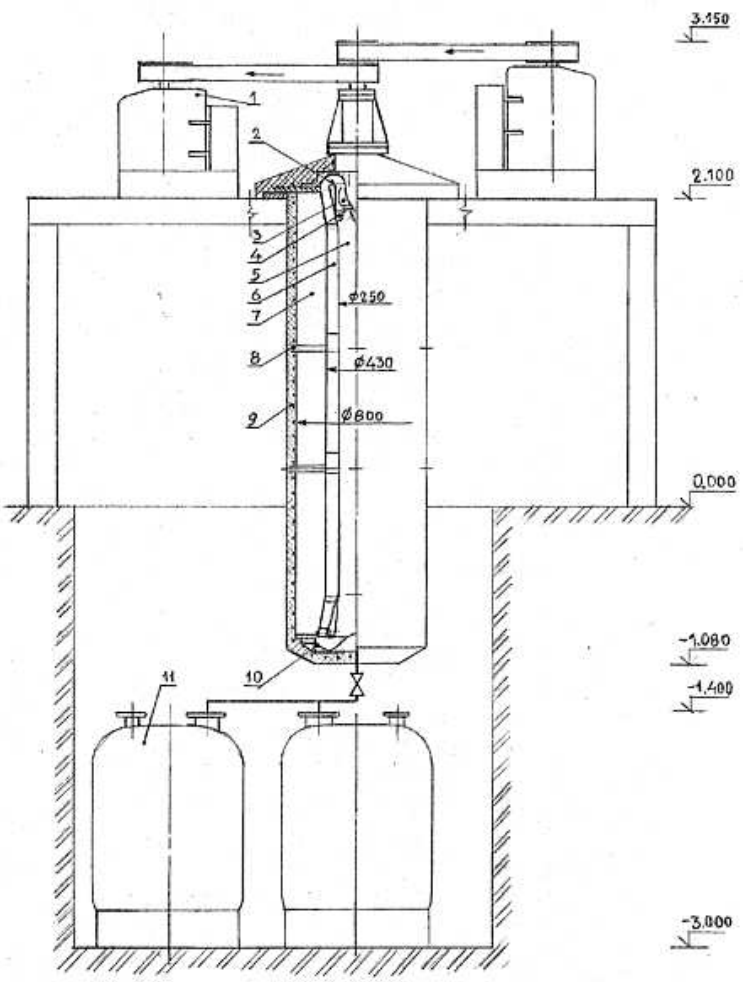

Figure 1. The experiment. 1 – DC motors 2 – pre-propeller vanes, 3 – propeller, 4 – post-propeller vanes, 5 – principal channel with swirling flow, 6 – channel with straight counterflow, 7 – immobile sodium, 8 – mechanical supports with field sensors inside, 9 – heaters with thermo-insulation, 10 – flow reversing guides, 11 – sodium storage

characterizing the relation between the averaged axial and azimuthal velocity. Restricting the following considerations on this Rm-oriented optimization, the power necessary for self-excitation must be kept in mind as the actual quantity to be minimized. Forcing a per se "optimal" velocity profile by means of too much leading blades can have a counterproductive effect.

3. One-dimensional calculations

Being interested only in the onset of the magnetic field self-excitation, we restrict ourselves in the following to the kinematic dynamo problem.
Combining Maxwell's equations and Ohm's law we find the induction equation for the magnetic field:

$$\frac{\partial \mathbf{B}}{\partial t} = -\frac{1}{\mu\sigma}\nabla \times (\nabla \times \mathbf{B}) + \nabla \times (\mathbf{v} \times \mathbf{B}) \; . \tag{4}$$

For the one-dimensional approximation we assume the velocity profile to be axisymmetric and independent of z:

$$\mathbf{v}(\mathbf{r}) = (0, v_\phi(r), v_z(r)) \; . \tag{5}$$

For the magnetic field we can make the ansatz

$$\mathbf{B}(r,\phi,z,t) = \left(\tilde{B}_r(r,t), \tilde{B}_\phi(r,t), \tilde{B}_z(r,t)\right) exp(im\phi + ikz). \tag{6}$$

Then the induction equation can be written in the following form:

$$\begin{aligned}
\frac{\partial \tilde{B}_r(r,t)}{\partial t} &= \frac{1}{\mu\sigma}\left[\left(\frac{1}{r}\frac{\partial}{\partial r}r\frac{\partial}{\partial r} - \frac{1}{r^2} - \frac{m^2}{r^2} - k^2\right)\tilde{B}_r(r,t) - \frac{2im}{r^2}\tilde{B}_\phi(r,t)\right] \\
&\quad - \left(\frac{im}{r}v_\phi + ikv_z\right)\tilde{B}_r(r,t) \qquad (7) \\
\frac{\partial \tilde{B}_\phi(r,t)}{\partial t} &= \frac{1}{\mu\sigma}\left[\left(\frac{1}{r}\frac{\partial}{\partial r}r\frac{\partial}{\partial r} - \frac{1}{r^2} - \frac{m^2}{r^2} - k^2\right)\tilde{B}_\phi(r,t) + \frac{2im}{r^2}\tilde{B}_r(r,t)\right] \\
&\quad - \left(\frac{im}{r}v_\phi + ikv_z\right)\tilde{B}_\phi(r,t) - \left(\frac{v_\phi}{r} - \frac{\partial v_\phi}{\partial r}\right)\tilde{B}_r(r,t) \qquad (8) \\
\frac{\partial \tilde{B}_z(r,t)}{\partial t} &= \frac{1}{\mu\sigma}\left(\frac{1}{r}\frac{\partial}{\partial r}r\frac{\partial}{\partial r} - \frac{m^2}{r^2} - k^2\right)\tilde{B}_z(r,t) \\
&\quad - \left(\frac{im}{r}v_\phi + ikv_z\right)\tilde{B}_z(r,t) + \frac{\partial v_z}{\partial r}\tilde{B}_r(r,t) \; . \qquad (9)
\end{aligned}$$

At all interfaces and boundaries the two tangential components of the electric and all three components of the magnetic field are demanded to be continuous.
A central difference scheme is applied for the space dependent part of the differential equation inside the system. For the outer part, modified Bessel functions are used and matched via the boundary conditions to the solution in the inner part. Concerning the time dependence, the 1D code is realized as a Crank-Nicolson scheme.

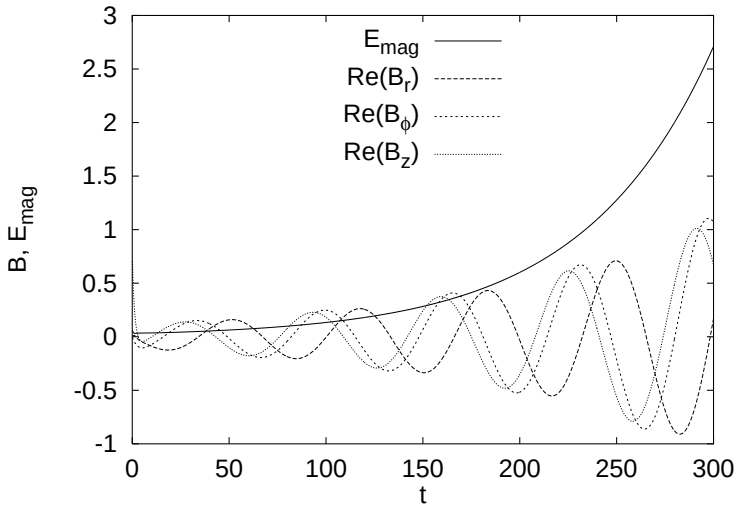

Figure 2. Time dependence of the the magnetic field components and the total magnetic energy (Ponomarenko flow).

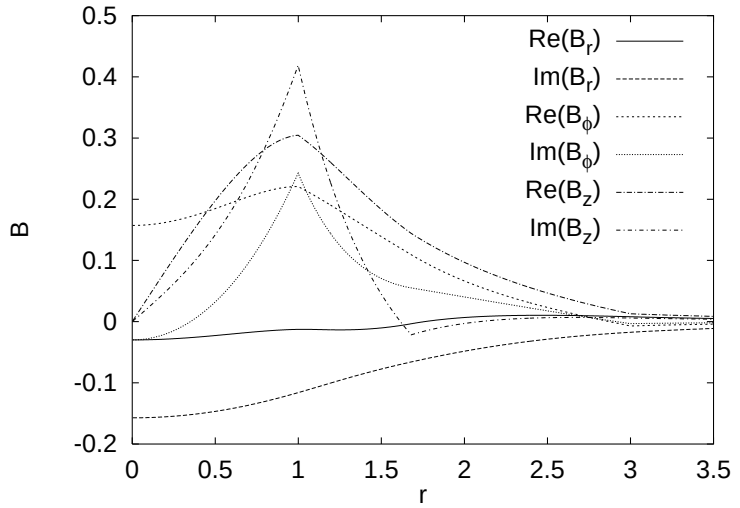

Figure 3. Radial dependence of the magnetic field components (Solid body rotation flow).

For the special case of a Ponomarenko flow figure 2 shows a typical time evolution of the real parts of the magnetic field (at a given r), and of the

total magnetic energy. Rm is chosen slightly above the critical value. Therefore, after the decline of an imposed seed field at the very beginning, an exponentially growing oscillation can be detected.
As an example of the resulting eigenstates, figure 3 shows the radial dependence of the magnetic field components for the solid body rotation profile. The relation of the three cylinder radii is, according to the experiment, 1.0 : 1.68 : 3.0.
Once the eigenstate of the magnetic field is reached its time evolution can be written in the form

$$\mathbf{B}(r,t) = \mathbf{B}_o(r)\ exp(p(Rm,k)t) \tag{10}$$

with a (complex) growth factor p depending on Rm and the wave number k. Then, the critical Rm for the convective instability, Rm^*, can be determined as the leftmost point of the so-called neutral curve which is the solution of

$$Real(p(Rm,k)) = 0\ . \tag{11}$$

Rm^{**}, the critical Rm for the absolute instability of the infinite length system, can be determined as the Rm where the (complex) group velocity

$$v_{group} = i\ \frac{\partial p(Rm,k)}{\partial k} \tag{12}$$

vanishes (for details see [8]). However, the most important critical Rm is Rm^{***} denoting the absolute instability for the real system of finite length (global instability). In principle, it can be estimated in the framework of a one-dimensional calculation, too [8]. We will mainly use the 2d code for its determination.
The results of this described 1D time evolution code were verified in part by an older 1D code developed by one of the authors (A.G.), which uses modified Bessel functions or polynomial expressions in the various cylinders and solves the nonlinear matching equations for these functions at the inner and outer boundaries.

4. Two-dimensional calculations

In order to check the effect of the finite length of the system and of possible variations of the velocities along the z-axis on the self-excitation threshold it was indicated to complement the one-dimensional results with two-dimensional calculation. In contrast to systems which can be embedded in spheres without major loss of accuracy, the Riga dynamo must be treated as a cylindrical problem due to its high aspect ratio.
At least in the redirection zones, the z-dependence of the velocity as well

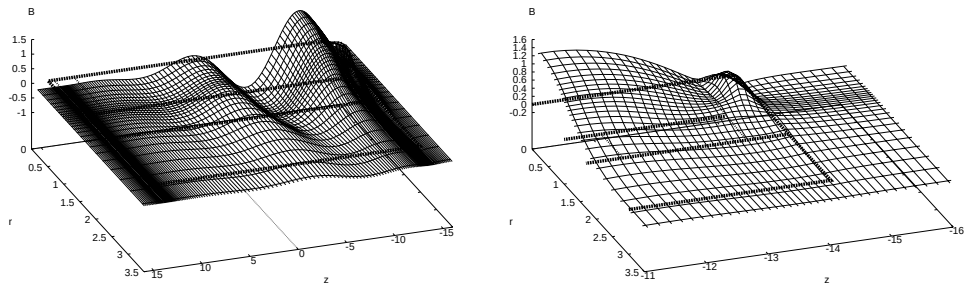

Figure 4. $Real(B_r(r,z))$ for the solid body rotation profile resulting from a 2d calculation. The thick lines delineate different flow zones. The helical flow in the innermost cylinder is located between $r = 0$ and $r = 1$. The propeller is on the left, driving the helical flow to the right. Left: overall picture. Right: details at the lower redirection zone.

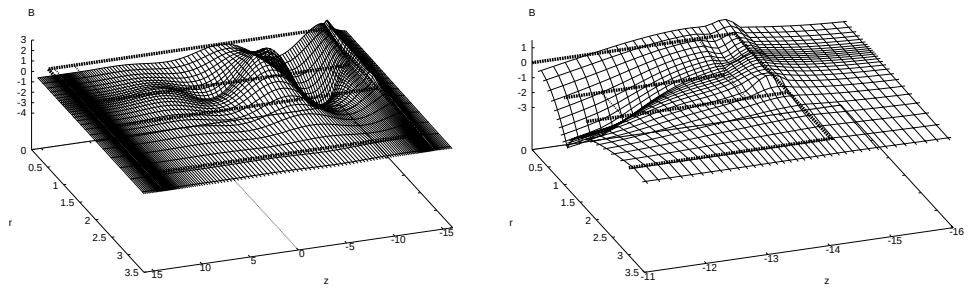

Figure 5. Same as figure 4 for $Real(B_\phi(r,z))$

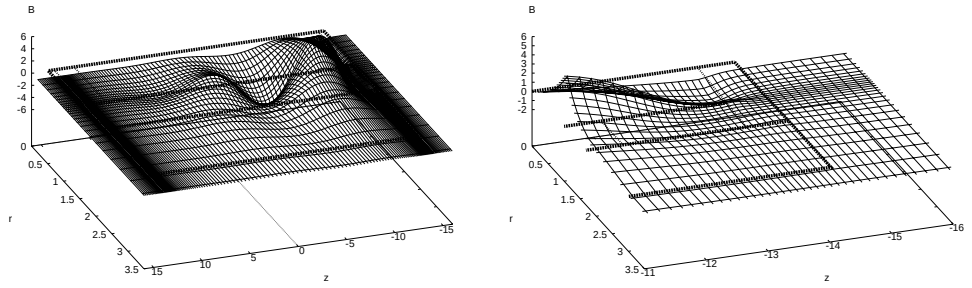

Figure 6. Same as figure 4 for $Real(B_z(r,z))$

as its v_r-component must be taken into account according to

$$\mathbf{v}(\mathbf{r}) = (v_r(r,z), v_\phi(r,z), v_z(r,z)) \ , \tag{13}$$

and the magnetic fields must be treated as z-dependent ones:

$$\mathbf{B}(r,\phi,z,t) = \left(\tilde{B_r}(r,z,t), \tilde{B_\phi}(r,z,t), \tilde{B_z}(r,z,t)\right) exp(im\phi) \ .$$

We omit the precise form of the induction equation. It can be derived from (7)-(9) replacing the terms $-k^2\tilde{B}_*$ by $\partial^2\tilde{B}_*/\partial z^2$ and adding several terms including v_r and its derivatives.
Again, a central difference scheme is applied for the space dependent parts. Non-uniform grid spacing is used in order to improve the resolution in the critical redirection zones of the flow. A slight rectangular simplification of the real geometry is necessary and the velocity in the redirection zones is approximated in an appropriate manner.
The time evolution is realized as an explicit Adams-Bashforth method of second order. The Laplace equation in the outer part is solved during every time step using a pseudo-transient method [9]. Indeed, this procedure is very time consuming during the first time steps. When the time evolution has reached a state close to the eigenstate of the induction equation, the pseudo-transient method can be speeded up enormously by multiplying the fields in the outer part first at all with a phase factor extracted from the inner part. However, it has to be noted that the total time necessary to reach the eigenstate is much longer than for the one-dimensional code since the large aspect ratio of the system leads to a long characteristic diffusion time.
In order to get an impression of the resulting fields, figures 4-6 show the three field components for the special case of a solid body rotation profile with $\kappa = 1$. The boundaries of the system as well as the interfaces between different flow regions are delineated with thick lines. The propeller is situated at the left. The magnetic fields are oscillating with an amplitude growing in flow direction.

5. Comparison of various velocity profiles

Although a wide variety of theoretical and measured velocity profiles has been considered, we restrict ourselves in the following to five representative profiles. For these profiles the first two rows of table 1 show the shape of the axial and azimuthal velocity components in the innermost cylinder. The relation between the radius R_1 of the innermost cylinder, the radius R_2 of the counterflow cylinder, the radius R_3 of the outermost cylinder and the length L of the apparatus is $R1 : R2 : R3 : L = 1.0 : 1.68 : 3.0 : 25.0$. All the profiles are assumed to be completed by a purely axial and constant counterflow. We tested also a number of counterflow profiles with azimuthal velocity components and a non-constant axial component. However, in view of the difficulties to maintain such profiles along the upward flow we con-

sidered a purely axial and constant counterflow as most appropriate for the experiment.
The critical Rm-values are determined either by means of the above mentioned 1D eigenvalue equation solver (a) and/or the 1D time-evolution code (b) or the 2D time-evolution code (c). Additionally, figure 7 shows the de-

TABLE 1. Critical Rm for the considered velocity profiles

	SBR	BEF	NGB	WGB	TGB
v_z	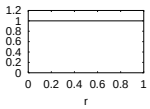	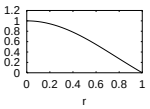	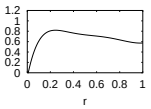	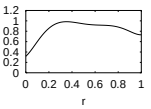	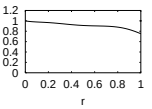
v_ϕ	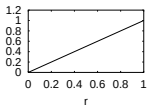	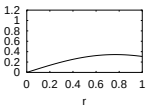	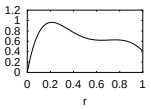	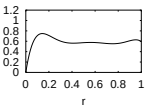	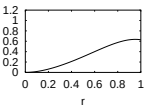
κ	1.00	1.20	0.73	1.10	1.30
Rm^*	$14.9^{a,b}$	$12.0^{a,b}$	25.6^b	17.0^b	14.3^b
Rm^{**}	$16.1^{a,b}$	$13.2^{a,b}$	27.6^b	18.3^b	15.7^b
Rm^{***}	$18.0^{a,c}$	$14.7^{a,c}$	31.0^c	21.5^c	17.6^c

pendence of Rm^* on the parameter κ (computed with method b).
The first profile represents the solid body rotation profile (SBR), which was assumed in former calculations, too. The second profile (BEF) requires some explanatory remarks: It is widely believed that helicity is effective in promoting the dynamo effect. Therefore, it is indicated to test velocity profiles with maximal helicity H for a given Rm (defined in (1)). The helicity is given as

$$\begin{aligned} H &= 2\pi\, L \int_0^R \mathbf{v}(r) \cdot \nabla \times \mathbf{v}(r)\, r dr \\ &= 2\pi\, L \int_0^R \left(v_z(r) \frac{\partial v_\phi(r)}{\partial r} + \frac{v_z(r) v_\phi(r)}{r} - v_\phi(r) \frac{\partial v_z(r)}{\partial r} \right) r dr \,. \end{aligned} \quad (14)$$

Bessel functions are resulting from the calculus of variation. Thus, the v_z- and the v_ϕ-component of the second profile (BEF) are given by the following expressions:

$$v_z(r) = \kappa\, J_0(2.4\, r) \quad (15)$$

$$v_\phi(r) = 1/\sqrt{2}\, J_1(2.4\, r) \,. \quad (16)$$

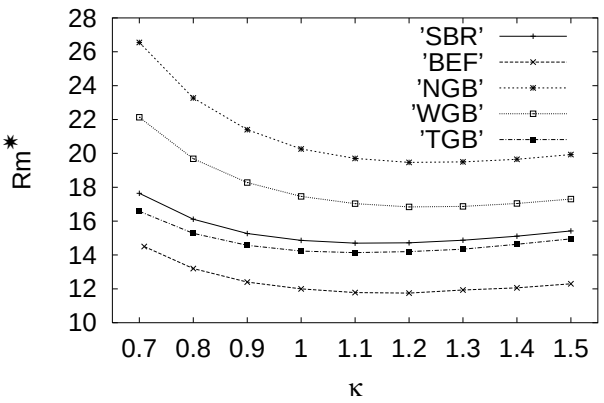

Figure 7. Dependence of Rm^* on the pitch parameter κ

The factor $1/\sqrt{2}$ in front of J_1 ensures (for $\kappa = 1$) helicity maximization for our somewhat "skew" expression $\overline{v_z}^2 + 2\,\overline{v_\phi}^2$. The Factor 2.4 in the argument of the Bessel functions is the maximal Lagrangian parameter used in the calculus of variation that ensures positivity of both velocity components in the innermost cylinder. Indeed, the critical Rm-values for these helicity maximizing profiles are the lowest we were able to find. Although the minimum of Rm^* is achieved for $\kappa = 1.2$ rather than for $\kappa = 1.0$, this result underlines the important role of helicity for the dynamo effect.
For the following discussion it is important to note that with the installed motors a Rm of the order of 22 can be achieved (depending slightly on the profile).
The third profile was measured in a first water experiment, where only a propeller and no guiding blades (NGB) were used[3]. All critical Rm are larger than the achievable Rm. The curve NGB in Figure 7 shows that these very high critical Rm are in part due to the small value of the pitch parameter ($\kappa = 0.73$), but the unfavourable shape of the profile is also responsible for that.
In order to avoid the over-rotation, guiding blades were welded into the upper turn-round in front of the propeller. The resulting profile with guiding blades (WGB) yields already much lower critical Rm-values. However, the WGB-profile still showed a serious defect of the axial velocity close to the axis which represented a disadvantage for the self-excitation as can be seen by comparison with the BEF-profile. To overcome this additional blades

[3]The measurements were carried out by means of a pressure probe. It should be noted that the measured values close to the axis may be not very accurate [10].

behind the propeller were necessary.
The fifth profile (two guiding blades: TGB) represents the velocity values

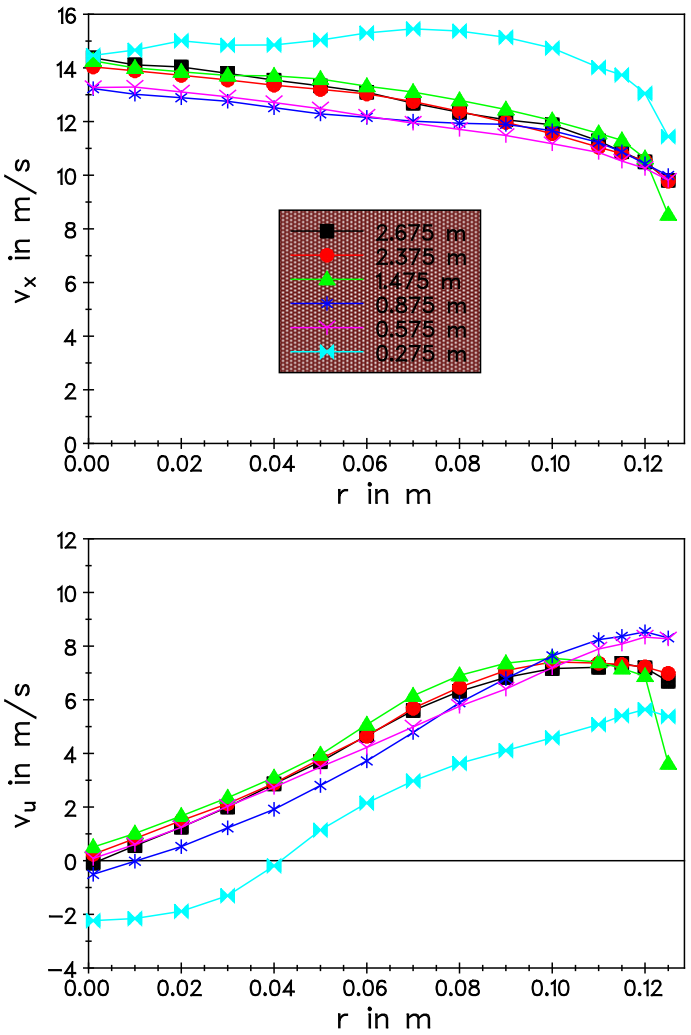

Figure 8. Velocity profiles measured for an propeller rotation rate of 1900 rpm depending on the distance from the propeller. Pre- and post-propeller blades are installed. Above: axial velocity versus radius. Below: azimuthal velocity versus radius.

which were measured after these additional guiding blades had been installed. [10]. As a matter of fact, the profile (TGB) is a mean representative of the really measured velocities at different distances from the propeller (see figure 8) The corresponding Rm-values are even a bit lower than the SBR values.

6. Conclusions

The real shape of the velocity profiles in the Riga dynamo experiment has a serious influence on the critical Rm. For helicity maximizing profiles the critical Rm can be reduced by 20 per cent compared to the corresponding value for the solid body rotation profile. This represents an important feature of the experimental design since the necessary power scales approximately with Rm^3. For all considered profiles, Rm^* has a minimum for κ close to 1.1. Thus, high helicity and a suitable pitch parameter are both important for the optimization of the velocity profiles.
The experimental velocity profiles in a water dummy channel have been improved by constructive changes. Whereas the propeller alone yields profiles which would by no means lead to self-excitation, the improvement by adding pre- and post-propeller blades leads eventually to velocity profiles giving a serious hope that self-excitation can be reached in the Riga sodium experiment.

Acknowledgments

This work was supported by Deutsche Forschungsgemeinschaft under INK 18/A1-1.
We would like to thank Prof. G. Will, M. Christen and H. Hänel from the Technical University of Dresden for designing the propeller and guiding vanes and measuring the velocity profiles.

References

1. Lowes, F. J. and Wilkinson, I (1968) Geomagnetic Dynamo: An improved Laboratory Model, *Nature*, **219**, pp. 717-718
2. Gailitis, A.K., Karasev, B.G., Kirillov, I.A., Lielausis, O.A., Luzhanskii, S.M., Ogorodnikov, A.P. and Preslitskii, G.V. (1987) Liquid metal MHD dynamo model experiment, *Magnitnaya Gidrodinamika* **4**, pp. 3-7
3. Gailitis, A. (1993) Experimental Aspects of a Laboratory Scale Liquid Sodium Dynamo Experiment, in: *Theory of Solar and Planetary Dynamos* (eds. M.R.E. Proctor, P.C. Matthews and A.M. Rucklidge), Cambridge University Press, pp. 91-98
4. Ponomarenko, Yu. B. (1973) On the theory of hydromagnetic dynamos, *Zh. Prikl. Mekh. Tekhn. Fiz.*, **6**, pp. 47-51
5. Gailitis, A. (1996) Project of a liquid sodium MHD dynamo experiment *Magnitnaya Gidrodinamika* **32**, pp. 63-67
6. Stieglitz, R. and Müller, U. (1996) GEODYNAMO - Eine Versuchsanlage zum Nachweis des homogenen Dynamoeffektes, Forschungszentrum Karlsruhe, Wissenschaftliche Berichte, FZKA 5716
7. Christen, M., Hänel, H., Will, G. (1998) Entwicklung der Pumpe für den hydrodynamischen Kreislauf des Rigaer "Zylinderexperimentes", To appear in: *Beiträge zu Fluidenergiemaschinen* **4**, Faragallah-Verlag und Bildarchiv
8. Gailitis, A. K. and Freiberg, J. ZH. (1977) Calculation of helical flux dynamo-instability, Preprint Riga

9. Fletcher, C. A. J. (1991) Computational Techniques for Fluid Dynamics, Vol. I, Springer Berlin-Heidelberg, S. 208
10. Will, G. and Christen, M. (1997) private communication